Dielectric Dispersion in Water + 2-Hydroxypyridine Solid Mixtures

A. Szala and K. Orzechowski*

Faculty of Chemistry, University of Wrocław, 14 F. Joliot-Curie 14, 50-383 Wroclaw, Poland

Received: May 21, 2004; In Final Form: January 25, 2005

The complex electric permittivity was measured in water + 2-hydroxypyridine (2HP) solid mixtures as a function of concentration, temperature and frequency. Just after freezing of diluted mixtures, (mole fraction of 2HP < 0.2) pronounced dielectric dispersion in the MHz region was observed. The dispersion disappears on cooling between −30 and −40 °C in a first-order phase transition. The dispersion was explained in terms of the movement of a guest molecule (2HP) in a clathratelike structure of ice.

Introduction

Freezing of polar liquids usually leads to the restriction of a movement of molecules that reduces or eliminates the orientation polarization. When the movement is blocked, the low-frequency permittivity attains values between 2 and 3. It is a characteristic feature for most substances in solid phase. Despite this "normal" behavior, some substances do not lose orientational freedom after freezing. One class of solids with rotational freedom are "rotator-phases" where overall movement of molecules is almost as easy as in normal liquids. Such rotational freedom was discovered both for small molecules (HCl, HI, HBr[1−4]) as well as for larger ones (*tert*-butyl chloride, polisubstituted alkanes, penta- and hexasubstituted benzenes, lower alcohols, etc.[5−9]). Generally the rotator-phase is expected for globular-in-shape or disk-in-shape molecules. Relaxation time, activation energy, enthalpy and entropy do not differ considerably from those observed in liquids just before freezing. When temperature decreases, the rotator phase usually disappears in a phase transition.

Other examples of solids with molecules able to rotate are glasses.[5,10−13] The main difference between rotator-phases and glasses is large increase of the relaxation time after vitrification. Glasses can be treated as supercooled liquids with very high viscosity. Because the relaxation time is a function of viscosity, the dielectric dispersion is shifted toward low frequencies.

The dielectric properties of ice[14,15] are different from those observed in rotator phases and in glasses. Low-frequency permittivity is a monotonic function of temperature in the freezing region, but the relaxation time increases by a few orders of magnitude. The parameters describing the relaxation process (relaxation time, activation energy) strongly depend on the existence of impurities in the ice structure.[16,17] Broad basis for the dielectric theory of ice was given by Bjerrum,[18] and the detailed theory was developed by Debye, Onsager, Gränicher, Steinemann, and Jaccard.[19] Defects in ice structure allow reorientation of water molecules much easier than in the ideal ice crystal, where four hydrogen bonds would have to be broken before reorientation can occur. Diffusion of the defects in an ice crystal gradually facilitates polarization of a sample (a single defect may allow to reorient many water molecules). The difusionally controlled reorientation is time-consuming and hence, the relevant process is shifted to very low frequencies as compared to the relaxation in liquid water.

Special examples of solids with orientation freedom are clathrates. Powell, as quoted by Franks,[20] describes clathrates as "the structural combinations of two substances which remain associated not through strong attractive forces but because strong mutual binding of molecules of one sort makes it possible to firmly enclose the other". Many substances may play a role of a "host"; of which water−ice is the best known. The guest molecules in ice clathrates occupy almost spherical holes in the host lattice. If only the guest molecules are sufficiently small, they possesses considerable rotational freedom.[20−22] If the guest molecules interact with the host cage not only through the van der Waals forces but also by specific interactions, the movement of the guest could be blocked.

Despite a couple of examples given above, the rotational freedom in the solid state is not a very frequently observed phenomenon. Discovery and explanation of this property is interesting not only from a theoretical stand point but also for practical reasons.

Gas-hydrates attract recently great interest because of the relevance to the environmental problems. The most important are clathrates of small molecules of hydrocarbons. Possibility of a formation of clathrates of larger molecules is also interesting and important especially in the case of the water-soluble synthetic heterocyclic aromatic compounds (as pyridine derivatives) used as industrial solvents, dyes, explosives, pharmaceuticals, and pesticides.

This paper is devoted to the presentation and description of the dielectric properties of water + 2-hydroxypyridine (2HP) solid mixtures. In a similar system investigated before (water + 2-methylpyridine[23]) considerable dielectric dispersion linked with the movement of 2-methylpyridine in ice-clathrate cages was found. The 2HP molecule has a smaller van der Waals diameter; however, it possess groups capable of forming a hydrogen bond between the host and the guest. It seems interesting to examine the possibility of formation of clathrates in 2HP + water mixtures and movement of 2HP in the cage.

Experimental Section

Materials. 2-hydroxypyridine was obtained from Aldrich (purity 95%) and it was used without additional purification. Water was obtained by reverse osmosis and degassed. Mixtures were prepared at room temperature by weighing.

* Corresponding author. E-mail: orzech@wchuwr.chem.uni.wroc.pl. Fax +48(71) 3282348. Telephone +48(71)3757235.

10.1021/jp047802r CCC: $30.25
Published on Web 03/08/2005

DSC Measurements. For differential scanning calorimetric measurements (DSC) a Perkin-Elmer DSC7 calorimeter was used. Samples were prepared as capsules with mixture of required concentration. Speed of temperature scans both in cooling and in heating was 1 K/min.

Dielectric Measurements. *Dielectric measurements in the frequency range 0.1 kHz to 1 MHz* was performed by means of an HP 4284 A RLC bridge. The capacitor was made of stainless steel and teflon and consisted of two coaxial electrodes (diameters 10 and 6 mm of outer and inner electrodes respectively). The sample was filling the space between electrodes. The capacitor was housed in a large, thermostated cooper block and surrounded by a vacuum cylinder, to provide thermal insulation. Temperature was stabilized by UNIPAN 243 temperature controller. Evaporated nitrogen was used as a cooling medium. Temperature was measured by a thermocouple with the resolution of 0.1 K. Air capacitance and lead capacitance, necessary for calculation of permittivity, were obtained in a calibration using standards (air, *n*-heptane, 1,2-dichloroethane).

Dielectric measurements in the frequency range 1 MHz to 1 GHz were performed with a lumped capacitance method[24] by means of an HP 4191A RF Impedance analyzer. The sample holder (made of stainless steel and glass) was mounted on the end of a coaxial waveguide. Samples were of diameter 13 mm and of thickness 1 mm. The part of the waveguide with the sample was mounted in the copper block. Temperature insulation, stabilization, and cooling were similar to those described for the low-frequency apparatus. Before measurements, the equipment was calibrated using standards (air, *n*-heptane, 1,2-dichloroethane).

Procedure of the Dielectric Measurements. The sample holder was filled with the liquid sample of required concentration at room temperature. Then the temperature was rapidly lowered to −10 °C. Supercooling results in rapid freezing that protects against heterogeneity of the obtained solid sample. Measurements were made dynamically and the temperature was changing approximately at 0.2 K/min. A personal computer was used for control of the measurements and data collection.

Experimental Errors and Repeatability of Dielectric Measurements. At low frequencies (0.1 kHz to 1 MHz) resolution of the permittivity measurements was relatively high (±0.1%). The resolution at frequencies 1 MHz to 1 GHz depended on the range. For the frequencies $10 < f < 800$ MHz the resolution was approximately 0.5%, whereas in the remaining frequency range 2%. The absolute errors of the obtained results were much larger due to poor repeatability of the data. Cooling of the solid sample is associated with volume change. The rigid electrodes of the sample holder cannot follow the variation of the sample thickness producing air gaps between electrodes and sample.[15,23] The resultant error of the permittivity was estimated at ±15%. Despite a large absolute error, the qualitative properties (temperature and frequency characteristics) of the investigated materials were repeatable.

Results

DSC Measurements. Differential scanning calorimetry was done on water + 2HP mixtures as a function of solute concentration. An example of temperature−heat flow dependence obtained in the mixture containing 0.05 mole fraction of 2HP is presented in Figure 1.

In the cooling run, a sharp peak close to −20 °C is produced by freezing of the supercooled mixture. Close to −41 °C, a relatively small peak is related to some exothermic process. In the heating mode, the low-temperature peak is shifted only slightly, to −35 °C. Melting is manifested as a broad peak between −10 and 0 °C. In all the investigated concentrations, two peaks in cooling and two peaks in heating runs were observed. The shift between freezing and melting was relatively large, whereas the hysteresis in the low-temperature process is rather small. Table 1 summarizes the DSC measurements.

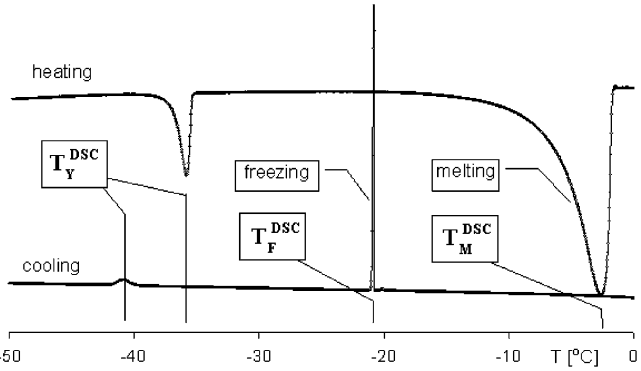

Figure 1. DSC measurements in water + 2HP mixture ($X_{2HP} = 0.05$): T_F^{DSC}, freezing temperature; T_M^{DSC}, melting temperature; T_Y^{DSC}, temperature of the second DSC peak observed both in cooling and in heating runs.

TABLE 1: Differential Scanning Calorimetric Measurements in Water + 2HP Mixtures as the Function of Solute Concentration[a]

	cooling run		heating run	
X_{2HP}	T_F^{DSC}	T_Y^{DSC}	T_Y^{DSC}	T_M^{DSC}
0	−11.0			0
0.01	−13.0	−41.0	−35.5	0.6
0.05	−20.8	−40.3	−37.7	−2.3
0.07	−21.2	−39.7	−34.6	−2.5
0.1	−25.7	−39.5	−34.8	−7.5

[a] Meaning of symbols: T_F^{DSC}, freezing temperature, T_M^{DSC}, melting temperature, and T_Y^{DSC}, temperature of the low-temperature peak in DSC measurements.

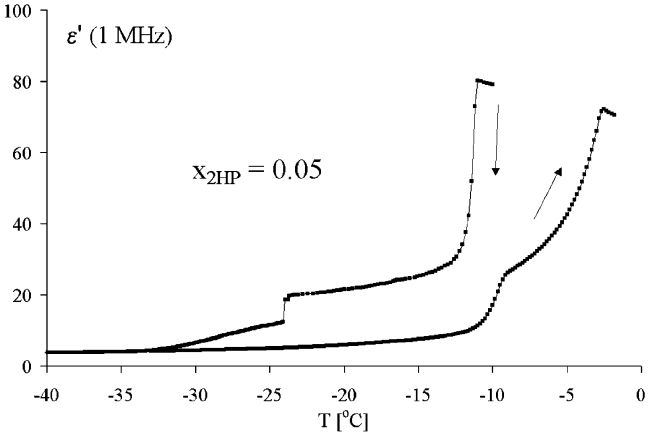

Figure 2. Electric permittivity in water + 2HP solid mixture ($X_{2HP} = 0.05$) vs temperature. Permittivity was measured at 1 MHz in coaxial capacitor using the low-frequency equipment.

Freezing temperature was found to decrease with rising 2HP concentration. The process at low temperature seems not to depend on the concentration.

Dielectric Measurements. *1. Temperature Dependence. a. Low Concentrations of 2HP ($x_{2HP} \leq 0.06$).* Figure 2 presents the temperature dependence of electric permittivity obtained at 1 MHz for a mixture containing 0.05 mole fraction of 2HP (data were obtained using the low-frequency equipment).

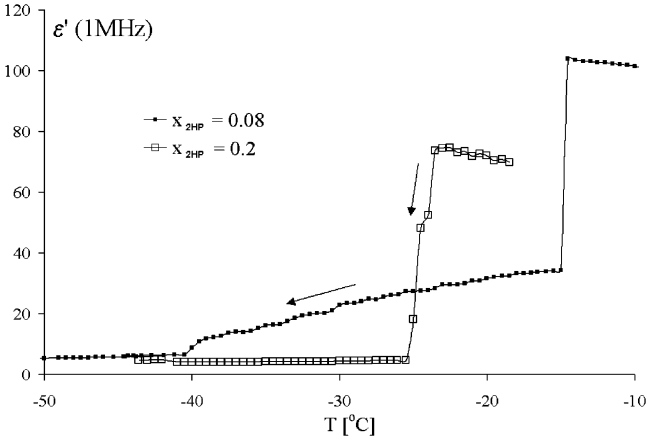

Figure 3. Electric permittivity in water + 2HP solid mixtures at high concentrations of 2HP vs temperature. Cooling curve for $X_{2HP} = 0.08$ mole fraction shows features similar to that for 0.05 mole fraction (Figure 2), but the low-temperature drop is less pronounced, separating a monotonically declining molecular polarization in the solid from the limiting low value of the distortion polarization. The cooling curve for 0.2 mole fraction exhibits no permittivity transition at all between the high value of molecular polarization in the liquid mixture and the limiting low value of the distortion polarization in the solid. Permittivity was measured at 1 MHz in coaxial capacitor using the low-frequency equipment.

In the cooling scan (Figure 2), the first permittivity downward jump occurs close to −12 °C. The jump marks freezing of the supercooled liquid mixture. In the temperature interval +12 to −24 °C the permittivity declines slowly, followed by a second jump down. With temperature dropping further, the permittivity gradually decreases to the value expected for ice at high frequencies (distortion polarization, which is not temperature dependent).

In the heating mode (Figure 2), permittivity increases very gradually to about −11 °C; at this point a steep rise occurs to a value observed in cooling mode between −12 and −24 °C. Following this upward jump, the permittivity increases rather steeply to a value characteristic of the liquid mixture.

The most characteristic and interesting feature of the cooling curve is the relatively high permittivity (20−25 units) registered in the −12 to −24 °C interval. It proves the existence of some orientational freedom in this temperature range, and it vanishes rapidly as the temperature keeps dropping below −24 °C.

For different samples the $\epsilon(T)$ dependence was similar to that shown in Figure 2, but absolute values were reproducible with rather poor precision (±15%). The temperature of the low-temperature jump also varied, even in successive runs with this same sample. These variations are function of cooling speed and the kinetics of spontaneous freezing of the supercooled mixture.

b. High Concentrations of 2HP ($x_{2HP} > 0.06$). The flat (or almost flat) $\epsilon(T)$ trend below freezing (Figure 2) was observed only for dilute mixtures (mole fraction of 2HP ≤ 0.06). For larger solute concentrations the temperature dependence was much steeper (e.g., 0.08 mole fraction, Figure 3). For the solute concentration $X_{2HP} = 0.2$ (Figure 3) freezing leads directly to the permittivity characteristic of ice at high frequencies.

2. Frequency Dependence. Most of the $\epsilon(f)$ dependences were investigated in the frequency range 1 MHz to 1 GHz. However, for selected concentrations the experiments were performed in the entire available range. The measurements shown in Figure 4 were made in the frequency range 0.1 kHz to 1 GHz for the sample containing 0.023 mole fraction of 2HP.

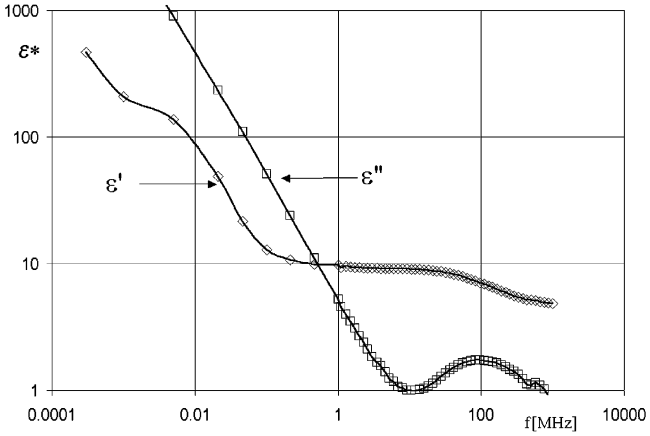

Figure 4. Real (ϵ') and imaginary (ϵ'') electric permittivity obtained in water + 2HP solid mixture ($X_{2HP} = 0.023$, $T = -20$ °C) as a function of frequency.

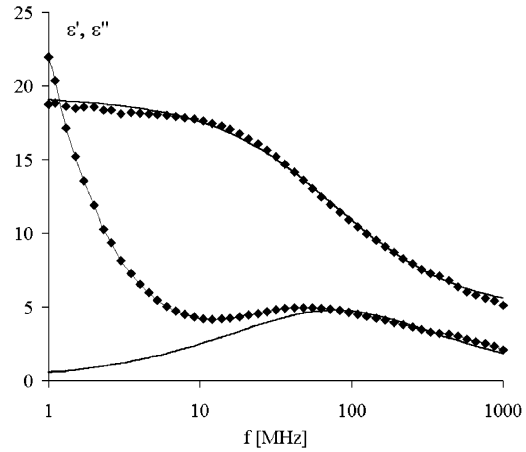

Figure 5. Real (ϵ') and imaginary (ϵ'') electric permittivities obtained in water + 2HP solid mixture ($X_{2HP} = 0.06$, $T = -20$ °C) as a function of frequency. Solid lines are fits to the Cole−Cole empirical function. The fitted $\epsilon''(f)$ dependence does not contain the conductivity term.

The $\epsilon'(f)$ dependence shows two distinct dispersions: one in the kilohertz and the second in the megahertz range. The low-frequency dispersion is attributed to dielectric relaxation of water molecules in ice or in icelike (perhaps clathratelike) structures. In pure ice, the dielectric relaxation time at −20 °C is 160 μs ($f_r \approx 1.0$ kHz).[15] However, in doped ice[16,17] and in clathrate structures[25,26,27] the relaxation time could be smaller. The observed increase of the permittivity at low frequencies is consistent with the expected relaxation. The ϵ'' between 10 MHz and 0.1 kHz rises at unity slope suggesting a static conductivity. (Figure 4 presents the ϵ'' data obtained for $f > 8$ kHz only; at lower frequencies the dependence is linear and was omitted for clarity) Large static conductivity seems to be a common feature of all the investigated samples. It considerably impedes the permittivity measurements in the area of low-frequency dispersion. The second dispersion was observed in the megahertz region. In pure ice, the electric permittivity in this range is approximately 3.1. We checked experimentally that the solid 2HP has, in this frequency range, a permittivity of approximately 4.5. Consequently it seems that the relaxation observed here is related to the special properties of water + 2HP solid mixtures.

Approximation of the High-Frequency Process. To present the frequency dependence of the permittivity in the dispersion range, an example of $\epsilon(f)$ obtained for the sample containing 0.06 mole fraction of 2HP at −20 °C is given in Figure 5.

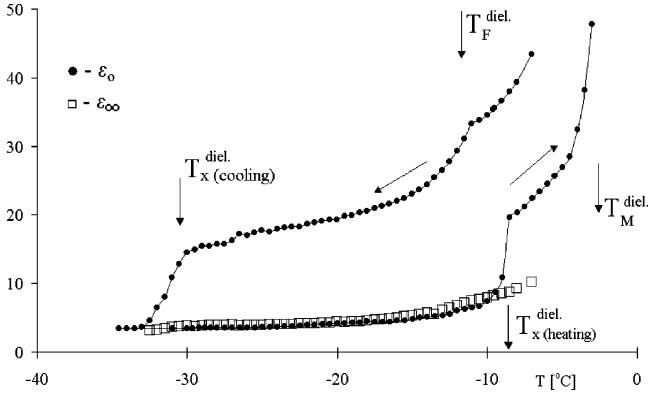

Figure 6. Temperature dependences of low-frequency and high-frequency limits of relative electric permittivity (ϵ_o and ϵ_∞ respectively) obtained in the fitting of the Cole−Cole equation to the data measured in the MHz range. The mole fraction of 2HP is 0.06. Meaning of the symbols: T_F^{diel}, freezing temperature; T_M^{diel}, melting temperature; T_X^{diel}-(cooling/heating), the temperature where orientational freedom is lost/recovered.

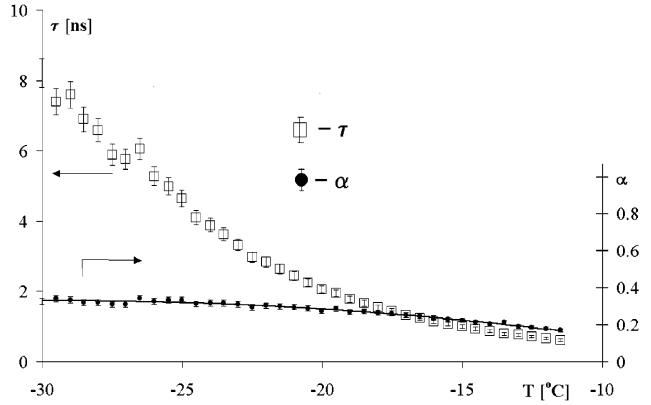

Figure 7. Macroscopic relaxation time (τ) and distribution parameter (α) obtained in the fitting routine vs temperature ($X_{2HP} = 0.06$, the Cole−Cole function).

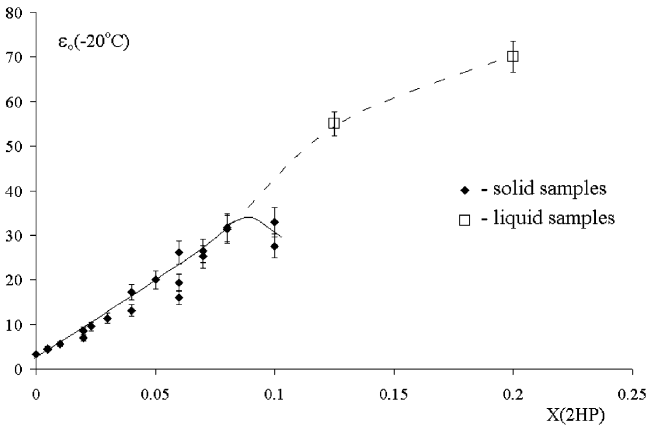

Figure 8. Static permittivity as a function of concentration, at −20 °C. Fit to the Cole−Cole empirical distribution.

The real part of the permittivity shows frequency dependence typical for the dispersion range, whereas ϵ'' increases strongly at lower frequencies. Linearity of $\epsilon''(f)$ dependence at low frequencies in log−log representation (as that presented in Figure 4) proves that it is caused by conductivity. The slope of $\epsilon'(f)$ dependence at $f < 10$ MHz may suggest some overlapping the low-frequency and high-frequency relaxations. However, strong conductivity makes difficult the investigations of the low-frequency process. Hence, we decided to describe the relaxation observed at f > 1 MHz as a single process with distribution of relaxation times. In the attempts of approximation, we tested Cole−Cole,[28] Davidson−Cole,[29] and Havrilak−Nagami[30] empirical functions with the conductivity term included ($i\sigma/\omega\epsilon_{fsp}$, where σ is DC specific conductivity, $\omega = 2\pi f$, and ϵ_{fsp} is the permittivity of a free space). The main difficulty impeding the precision of the calculations was the absence of the high-frequency limit of the permittivity. It leads to considerable uncertainty of the calculated parameters in the case of Davidson−Cole and Havrilak−Nagami functions, despite lower fitting errors in the last case. Taking into account the above, we used only the Cole−Cole empirical equation. As an example of the obtained results, we present the temperature dependence of the fitted parameters for the mixture containing 0.06 mole fraction of 2HP (Figure 6). The dependencies obtained at the remaining concentrations are qualitatively similar.

The temperature dependence of the fitted low-frequency limit of relative permittivity (ϵ_o) in the cooling run is similar to the dependence obtained at 1 MHz using the low-frequency bridge and coaxial capacitor. However, contrary to the experiments performed at 1 MHz, a saddle is shown (Figure 6) just below −12 °C where the freezing range ends. The existence or the absence of the saddle was found to be a function of cooling speed and the geometry of the capacitor. It could be the result of a solid−liquid equilibrium before the sample was completely frozen. According to Figure 6, in the temperature interval between −12 and −30 °C the calculated ϵ_o decreases slowly followed by rapid decrease below −30 °C. At low temperatures ϵ_o has a value of 3−4, similar to that for ice in the megahertz region. In the heating run, the permittivity dispersion was not observed and ϵ_o is almost equal to the ϵ_∞ obtained in a cooling mode. A pronounced ϵ_o jump and "return" of the distinct dispersion was observed just before melting, close to −8 °C.

The high-frequency limit of permittivity (ϵ_∞) was found to decrease with the temperature. At low temperatures it attains the value (3.2 ±0.1), equal to that in pure ice.

The relaxation time, calculated from the data collected in the cooling run in the temperature range −12 to −30 °C, was found to increase with decreasing of temperature (Figure 7). It was found, that the relaxation time follows the Eyring formula: $\ln(\tau T) = A + \Delta H^*/(RT)$.

The distribution parameter α, is relatively large and increases with a decreasing temperature. At −15 °C, its value is approximately 0.15, and at −30 °C, it attains 0.3. The large value of this parameter reflects probably some overlapping of the low-frequency and high-frequency processes.

The dependencies of the fitted parameters in other samples were qualitatively similar. Figure 8 presents the values of ϵ_o obtained at −20 °C in all the investigated samples.

At −20 °C for concentrations smaller than $X_{2HP} = 0.08$, ϵ_o increases monotonically with concentration, but at larger concentrations some decrease was observed. It is interesting that in Figure 8 extrapolation of the $\epsilon_o(X_{2HP})$ dependence observed in solid ice + 2HP samples seems to grade into the permittivities obtained in liquid samples at higher concentrations. However, it has to be stressed that the analyzed solid samples did not indicate (macroscopically) the existence of liquid phases. Table 2 summarizes the results of dielectric and DSC measurements obtained in the cooling runs in all the investigated samples.

Discussion

The most characteristic property of the investigated water−2HP mixtures is the existence of two dispersion regions, one in

TABLE 2: Collected Results of the Dielectric and DSC Measurements

X_{2HP}	T_F^{diel} [°C][a]	T_X^{diel} [°C][b]	T_F^{DSC} [°C][c]	T_Y^{YDSC} [°C][c]	ϵ_o (−20 °C)[d]	ϵ_∞ (−20°C)[d]	α (−20 °C)[d]	τ [ns] (−20 °C)[d]	E_A [kJ/mol][e]
0.005	−11 to −15	−22 to −30	−12.2	−41.2	4.3−4.4	3.0	0.5	0.3	48
0.01	−16	−22	−12.9	−41.1	5.7	3.3	0.4	1.1	37
0.02	−14	−22 to −23	−14.4	−41.0	7.0−8.2	3.5	0.2	1.6	48
0.023		−23	−14.8	−40.9	9.3	4.6	0.2	1.5	61
0.03	−10 to −17	−22 to −26	−15.8	−40.8	9.0−15.0	3.8	0.3	1.3	73
0.04	−16 to −17	−28 to −30	−17.3	−40.6	13.1−17.4	3.9	0.2	2.1	78
0.05	−17	−30	−18.7	−40.4	21.1	5.3	0.2	2.0	70
0.06	−11 to −13	−22 to −32	−20.2	−40.3	19.3−26.0	4.4	0.3	2.1	74
0.07	−16 to −17	−22 to −35	−21.6	−40.1	25.2−26.0	4.6	0.3	2.4	35
0.08	−15 to −17	−27 to −40	−23.1	−39.9	30.7	5.1	0.3	2.1	63
0.1	−16 to −17	−23	−26.0	−39.6	27.6−33.0	5.3	0.3	2.0	92
0.125	−33	−40			55[f]				
0.2		−17			70[f]				

[a] T_F^{diel} is the range of temperatures where the first permittivity jump was observed when obtained in the cooling run. [b] T_X^{diel} is the range of temperatures where the second permittivity jump was observed (cooling run). Between T_X^{diel} and T_F^{diel}, dielectric dispersion and absorption were observed. [c] T_F^{DSC} and T_Y^{DSC} are the freezing temperature and temperature of the low-temperature peak interpolated from DSC measurements. [d] ϵ_o, ϵ_∞, α, and τ are, respectively, the static relative permittivity, high frequency limit for the relative permittivity, distribution parameter, and macroscopic relaxation time. These parameters were calculated after fitting of the Cole−Cole empirical equation to the data obtained at −20 °C. [e] E_a − activation energy of the dielectric process observed between T_F^{diel} and T_X^{diel} calculated according to the Eyring formula: $\ln(T\cdot\tau) = E_a/(R\cdot T) + B$. [f] Permittivity in liquid phase.

kilohertz and the second in megahertz regions. The first one (kilohertz dispersion) is observed even in pure ice and will not be considered here. The second process (megahertz dispersion) is observed at a temperature just below freezing of the mixture. Because neither in pure ice nor in pure 2HP solid samples, any dispersion was observed in this frequency range, we suppose that the dispersion reflects a special structure and properties of the investigated solid mixtures. The temperature range where the dispersion in solid H_2O + 2HP mixtures was observed is relatively small and it disappears between −30 and −40 °C. In heating, the transition to the phase where the dispersion is recovered, is shifted toward much higher temperatures. This large temperature shift suggest a first-order phase transition that is responsible for the disappearing and recovering of the relaxation. Both in the dielectric and in the DSC measurements, two characteristic temperatures were observed in both cooling and heating curves. The high-temperature transitions in both experiments were explained as freezing and melting, respectively. The low-temperature DSC peaks usually were located at lower temperatures than those in the dielectric measurements. The temperature shift of DSC low-temperature peaks in cooling and in heating was relatively small, whereas the low-temperature transition shift in the dielectric measurements was very large (compare temperatures $T^{diel}_{X(cooling)}$ and $T^{diel}_{X(heating)}$ in Figure 6). We suspect that the low-temperature transition observed in DSC measurements reflects a process different from that of the dielectric response.

To explain the dielectric dispersion and absorption observed in cooling between $T^{diel}_{X(cooling)}$ and $T^{diel}_{X(heating)}$, it is interesting to consider the possibility of formation of ice clathrate structures. A geometry optimization of 2HP has been performed using the ab initio MP2 method. In the calculation the Gaussian 98 package the 6-311++G(d,p) basis set has been employed.[31] The obtained largest van der Waals diameter was found to be 6.5 Å. Large cages of structure II of ice clathrate (space group *Fd*3*m*, cell parameter 17.31 Å[32]) have the "free" diameter 6.6 Å.[20] The largest van der Waals diameter of the 2HP molecule seems to be a limiting value for the guest molecules in simple ice clathrate. However, it is found also that larger molecules can give clathrate structures.[20] To provide sizable host cages the complex polyhedron can be formed by combination of individual cavities. Such structures are characteristic for amines and hydroxyl compounds.[33−35] Hydrogen bonds between the host and the guest seem to stabilize such structures.[36] The 2,6-dimethylpyridine molecule has a slightly larger diameter (7.4 Å estimated by MP3 semiempirical method) than that obtained for 2HP. The 2,6-dimethylpyridine molecule was found to be located in cavities of *β*-trydyminite with the hydrogen bonding between the nitrogen and the host.[37]

TABLE 3: Comparison of the Data Obtained in Water + 2MP and Water 2HP Systems[a]

	2MP[23]	2HP
the largest van der Waals diameter [Å]	6.8[a]	6.6
$(\epsilon_o - \epsilon_\infty)_{x=0.05}$ at −20 °C	8.1	12
τ [ns]	0.65	2.5
ΔH [kJ/mol]	40±2	75±5

[a] In ref 23, the diameter estimated without auxiliary semiempirical calculation was found to be 8 Å.

The dielectric dispersion observed in the water + 2HP solid system investigated here could be linked with the reorientation of the guest molecule in the host cage. However, free rotation is hardly possible, except perhaps a movement conjugated with phonons. Many-body interactions and collective movement of host molecules may realize the rotation of the guest.[38,39] This model can explain the relatively small activation energy of strongly hindered rotation of guest molecules in a host lattice, which may account for our measurements in the water−2HP mixtures (see Table 2). The dispersion and absorption could also be treated as the result of a small-angle movement and/or librations of the encaged molecules in the rigid host lattice. However, to understand a large permittivity dispersion, mutual interaction between encaged molecules and a collective movement under the influence of an external field has to be supposed. Gavezzotti and Simonetta[40] demonstrated that the collective movement of at least 25 molecules could reproduce a large permittivity dispersion with relatively small activation energy.

Qualitative properties of the investigated system are similar to those observed previously in water + 2-methylpyridine (2MP) solid mixtures.[23] Table 3 compares the data obtained in water + 2MP and water 2HP systems.

The 2HP molecule has a smaller van der Waals diameter; however it possesses the −OH group capable of forming a hydrogen bond between the host and the guest. This results in considerably increased relaxation time and activation energy as compared with the water + 2MP system. In water + 2HP solid mixture the dispersion vanishes not lower than at −40

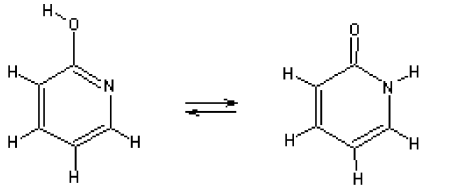

Figure 9. Tautomeric equilibrium between 2-hydroxypyridine and 2-pyrimidone.

°C. In the case of water + 2MP a pronounced dielectric dispersion was observed even at − 60 °C. The differences between those two systems probably result from the existence in the 2HP molecule of two groups capable of forming a hydrogen bond (−OH and nitrogen in the ring). The difference between activation enthalpy obtained for 2HP and for 2MP is 30 ± 8 kJ/mol, roughly consistent with the energy of a single hydrogen bond.

There is also another possibility for explaining the dispersion observed in the water + 2HP solid mixture. The 2HP molecule is a well-known example of keto−enol tautomerism (Figure 9).[41]

The tautomers have almost the same stability in the gas phase (free energy of 2HP is 3.2 kJ/mol lower than that of 2PD[42]). The keto-form has a much larger dipole moment. The MP3 semiempirical calculation gives the dipole moment 3.69 D for 2PD and only 1.24 D for 2HP. The less polar 2HP is favored in gas phase and in solvents of low permittivity, whereas 2PD dominates in polar solvents. The equilibrium between tautomers is a consequence of a proton movement between oxygen and nitrogen. It was found that the protic solvents, such as alcohols and water, considerably decrease the potential barrier between both tautomers. In gas phase the activation energy is relatively high (150 ± 10 kJ/mol), whereas it is reduced to about 58 ± 4 kJ/mol in the presence of bridging water molecules.[43,44] The keto−enol tautomerism may account for the dispersion and absorption characteristics observed in the investigated system. In the course of solidification the 2HP molecules were incorporated into the ice structure, probably into the ice clathrate—as was substantiated above. Considerable absorption and dispersion in the solid water + 2HP mixture could be explained as an ice-promoted proton movement resulting in equilibrium between both tautomers. The mean activation energy of 70 ± 5 kJ/mol obtained from dielectric measurements does not contradict this possibility.

Conclusions

The mixture of water + 2-hydroxypyridine (2HP) shows considerable dielectric dispersion and absorption just after freezing. The temperature range where the dispersion is observed is limited by the phase transition where rotational and/or librational freedom is lost. It was supposed that the formation of a clathratelike structure develops, with the 2HP molecule encaged in host water−ice cages. The parameters of the relaxation process (relaxation time, activation enthalpy, and dielectric increment) and the comparison with the previously investigated water + 2-methylpyridine solid mixtures seems to confirm the proposed mechanism. The 2HP molecule is probably hydrogen-bonded to the host lattice; this would increase the relaxation time and the activation energy.

An alternative explanation of the observed relaxation is as follows: the 2HP molecule is an example of keto−enol tautomerism. The dispersion could be a result of the chemical equilibrium between tautomers (2-hydroxypyridine and 2-pyrimidone), possible in the presence of bridging water molecules. This process could take place both in clathratelike structures and in amorphous solid mixture of 2HP and ice. Nevertheless, large similarities observed in dielectric properties of water + 2HP and in water + 2MP solid mixtures and a lack of any tautomeric equilibria in water + 2MP seem to favor the former relaxation mechanism.

Acknowledgment. We are very grateful to Dr. B. Czarnik-Matusewicz and Prof. Z. Pawełka for the quantum-mechanical and semiempirical calculations.

References and Notes

(1) Cole, R. H.; Havrilak, S. *Discuss. Faraday. Soc.* **1951**, *23*, 31.
(2) Philips, C. S. E. *J. Phys.* **1952**, *13*, 216.
(3) Brown, N. L.; Cole, R. H. *J. Chem. Phys.* **1952**, *20*, 196.
(4) Clausius, K.; Wolf, G. *Z. Naturforsch.* **1947**, *2A*, 495.
(5) Smyth, C. P. *Dielectric Behaviour and Structure*; McGraw-Hill Book Company, INC, New York − Toronto − London, 1955.
(6) White, A. H.; Biggs, B. C.; Morgan, S. O. *J. Am. Chem. Soc.* **1940**, *62*, 16.
(7) Brot, G.; Darmon, I. *J. Chim. Phys. 63* **1966**, 100.
(8) Cataliotti, R. S.; Paliani, G.; Sorriso, S. *J. Chem. Phys.* **1986**, *85*, 5587.
(9) Kołodziej, H. A.; Orzechowski, K.; Szostak, R.; Sorriso, S. *J. Mol. Struct.*, **1995**, *344*, 183.
(10) Turkevich, A.; Smyth, C. P. *J. Am. Chem. Soc.* **1942**, *64*, 737.
(11) Stickel, F.; Berger, T.; Richert, R.; Fisher, E. W. *J. Chem. Phys.* **1997**, *107*, 1086.
(12) Paluch, M.; Zioło, J.; Rzoska, S. J. *Phys. Rev.* E. **1997**, *56*, 5764.
(13) Park, I. S.; Saruta, K.; Kojima, S. *J. Phys. Soc. Jpn.* **1998**, *67*, 4131.
(14) Smyth, C. P.; Hitchcock, S. C. *J. Am. Chem. Soc.* **1932**, *54*, 4631.
(15) Auty, R. P.; Cole, R. H. *J. Chem. Phys.* **1952**, *20*, 1309.
(16) Kawada, S.; Jin, R. G.; Abo, M. *J. Phys. Chem.* **1997**, *101*, 6223.
(17) Takei, I.; Maeno, N. *J. Phys. Chem.* **1997**, *101*, 6234.
(18) Bjerrum, B. *Science* **1952**, *115*, 385.
(19) Petrenko, V. F.; Whitworth, R. W. *Physics of Ice*; Oxford University Press: Oxford, U.K., 1999; Chapter 4.
(20) *Water, a Comprehensive Treatise*; Franks, F., Ed.; Plenum Press: New York and London, 1973; Vol. 2.
(21) Jacobs, D. M.; Zaidler, M. D.; Kanert, O. *J. Phys. Chem. A* **1997**, *101*, 5241.
(22) Horikawa, S.; Itoh, H.; Tabata, J.; Kawamura, K.; Hondoh, T. *J. Phys. Chem. B* **1997**, *101*, 6290.
(23) Orzechowski, K.; Marczak, W.; Ernst, S. *J. Mol. Struct.* **1995**, *415*, 45.
(24) Kolodziej, H. A.; Pajdowska, M.; Sobczyk, L. *J. Phys. E* **1978**, *11*, 752.
(25) Hawkins, R. E.; Davidson, D. W. *J. Phys. Chem.* **1966**, *70*, 1889.
(26) Venkateswaran, A.; Easterfield, J.; Davidson, D. W. *Can. J. Chem.* **1967**, *45*, 884.
(27) Morris, B.; Davidson, D. W. *Can. J. Chem.* **1971**, *49*, 1243.
(28) Cole, K. S.; Cole, R. H. *J. Chem. Phys.* **1941**, *9*, 341.
(29) Davidson, D. W.; Cole, R. H. *J. Chem. Phys.* **1950**, *18*, 1417.
(30) Havrilak, S.; Nagami, S. *J. Polym. Sci., Part C: Polym. Symp.* **1966**, *14*, 99.
(31) *Gaussian 98, Revision A.9*. Gaussian, Inc.: Pittsburgh, PA, 1998.
(32) Jeffery, G. A.; McMullan, R. K. *Prog. Inorg. Chem.* **1967**, *8*, 43.
(33) Feil, D.; Jeffery, G. A. *J. Chem. Phys.* **1961**, *35*, 1863.
(34) Mak, T. C. W. *J. Chem. Phys.* **1965**, *43*, 2799.
(35) McMullan, R. K.; Jeffery, G. A.; Jordan, F. H. *J. Chem. Phys.* **1967**, *47*, 1229.
(36) Glew, D. N. *Trans. Faraday Soc.* **1965**, *61*, 30.
(37) Wegner, E.; Wieder, J.-U.; Zimmerman, H. W. *Ber. Bunsen-Ges. Physik Chem.* **1976**, *80*, 405; **1977**, *81*, 1143.
(38) Dissado, L. A.; Hill, R. M. *Chem. Phys.* **1987**, *111*, 193.
(39) Dissado, L. A.; Nigmatilin, R.; Hill, R. M. *Dynamical Processes in Condensed Matter*; Evans, M. R., Ed.; Advances in Chemical Physics 63; Wiley: New York, 1985.
(40) Gavezzotti, A.; Simonetta, H. *Acta Crystallogr., Sect. A* **1976**, *3*, 997.
(41) Beak, P. *Acc. Chem. Res.* **1977**, *10*, 186.
(42) Nowak, M. J.; Łapiński, L.; Fulara, J.; Leś, A.; Adamowicz, L. *J. Phys. Chem.* **1992**, *96*, 1562.
(43) Moreno, M.; Miller, W. H. *Chem. Phys. Lett.* **1990**, *171*, 475.
(44) Barone, V.; Adamo, C. *J. Phys. Chem.* **1995**, *99*, 15062.